Cement and Concrete Research 41 (2011) 38–45

Contents lists available at ScienceDirect

Cement and Concrete Research

journal homepage: http://ees.elsevier.com/CEMCON/default.asp

Evaluation of a low temperature hardening Inorganic Phosphate Cement for high-temperature applications

M. Alshaaer [a,*,1], H. Cuypers [b], G. Mosselmans [c,1], H. Rahier [d], J. Wastiels [b]

[a] Materials Research Laboratory, Deanship of Academic Research, University of Jordan, Amman 11942, Jordan
[b] Department of Mechanics of Materials and Constructions (MEMC), Vrije Universiteit Brussel (VUB), Pleinlaan 2, 1050 Brussels, Belgium
[c] Belgian Research Center of Cement Industry (CRIC-OCCN), Bld du Souverain 68, 1170 Brussels, Belgium
[d] Research Group of Physical Chemistry and Polymer Science (FYSC), Vrije Universiteit Brussel (VUB), Pleinlaan 2, 1050 Brussels, Belgium

ARTICLE INFO

Article history:
Received 5 July 2009
Accepted 7 September 2010

Keywords:
Temperature
Cement
Mechanical properties
Aging
Pore size distribution

ABSTRACT

Phase and mechanical changes of Inorganic Phosphate Cement (IPC) are identified along with changes in macro properties as functions of temperature and time. In addition to amorphous phases, the presence of significant amounts of brushite and wollastonite in the reference IPC is confirmed using X-ray diffraction. The thermal behavior of IPC up to 1000 °C shows that contraction of the solid phase in IPC due to chemical transformations causes reduction in the volume of the material. Also the ongoing meta-stable calcium phosphate transformations and reactions over a long time contribute significantly to the phase instability of the material at ambient conditions. It is found that the strength of IPC increases with ageing at ambient conditions but the formation microcracks below 105 °C causes a sharp reduction in the mechanical performance of IPC. According to the results obtained by Mercury intrusion porosimetry, the pore system of the reference IPC is dominated by mesopores.

1. Introduction

Calcium phosphate cement is the generic term to describe chemical formulations in the chemical system that can experience a transformation from a liquid or pasty state to a solid state, and in which the end product of the reaction is a calcium phosphate. These cements consist generally of a concentrated mixture of one or several calcium phosphate powders and an aqueous solution (e.g. water), but it may also consist of a mixture of two or more solutions [1,2]. These cements have the ability to precipitate different end products (e.g. hydroxyapatite, calcium deficient apatite, brushite, etc.) after full conversion [3]. The calcium phosphate cements (CPCs) are commonly used in dentistry and orthopedic bone filling surgeries, which require extremely invasive procedures [1–6]. The discovery of CPCs has been ascribed to Brown and Chow for an abstract published in 1983 [4]. However, several authors worked with similar reactions before 1983. For example, Kingery looked at formulations based on CaO and phosphoric acid in 1950 [5]. Over the last few years, researchers at the Vrije Universiteit Brussel (VUB) have been developing a chemically bonded Inorganic Phosphate Cement (IPC) for structural and industrial applications where (accidental) and high temperatures may occur. This material is called Inorganic Phosphate Cement (IPC) and is available under the commercial brand name Vubonite [7]. IPC is a new material that sets at room temperature, with unique properties for manufacturing E-glass fiber reinforced composite materials. Such a textile reinforced cementitious composite is an interesting material in those applications where high load-bearing capacity, good temperature or fire resistance, and lightweight constructions are demanded [8]. IPC is a two-component system, consisting of a calcium silicate powder and a phosphoric acid-based solution of metal oxides. After hardening, the material's properties are similar to those of Portland cement based materials. IPC can be used in elevated temperature applications such as moulds for shaping of composites with thermoplastic matrix or post curing of thermosets. Because the IPC belongs to a novel class of room-temperature-setting chemically bonded materials with remarkable thermal, structural and rheological properties that are ideal for matrices of fibre reinforced composite materials, the main objective of this paper is to study the impact of temperature and time on its properties. The thermal and dimensional stability of the material is evaluated in order to provide an overview of the main challenges that will be encountered when using IPC in various applications. Specifically, the problems which will limit the use of IPC in structural applications will be investigated and identified, particularly those related to heat resistance and ageing. A link between mechanical properties and molecular and microstructure is looked for.

2. Basic chemistry of IPC

The setting reaction of IPC was described in previous work [9]. A small overview will be given here. The reaction between the Ca source wollastonite ($CaSiO_3$) and the phosphoric acid solution starts in a very

* Corresponding author. Tel.: +962 776330873; fax: +962 6 5355599.
E-mail address: mazen72@yahoo.com (M. Alshaaer).
[1] Formerly at Department of Mechanics of Materials and Constructions (MEMC), Vrije Universiteit Brussel (VUB), Pleinlaan 2, 1050 Brussels, Belgium.

0008-8846/$ – see front matter © 2010 Elsevier Ltd. All rights reserved.
doi:10.1016/j.cemconres.2010.09.003

acidic environment (pH around 1). During the reaction, the pH increases, reaching about 7 at completion. For molar ratios P/Ca between 0.39 and 1, only one type of calcium phosphate (brushite, $CaHPO_4.2H_2O$) is formed. This reaction is represented in Eq. (1).

$$CaSiO_3 + H_3PO_4 + (1 + x)\,H_2O = SiO_2.xH_2O + CaHPO_4.2H_2O \quad (1)$$

Alongside brushite, also amorphous silica is formed as a result of the leaching out of Ca from the wollastonite. The Ca cations recombine with phosphate anions and the precipitation layers glue together the silica and remaining wollastonite particles. The first precipitate is amorphous and only in a later stage of the reaction crystalline brushite is formed.

Calcium phosphate phases (CaP) belong to the family of apatites. There are several CaP phases, the most ubiquitous being hydroxyapatite (HAp, $Ca_{10}(PO_4)6(OH)_2$). Other CaP structures include brushite (DCPD, $CaHPO_4.2H_2O$) and tricalcium phosphate (TCP, $Ca_3(PO_4)_2$). Several low- and high-temperature approaches have been reported for synthesizing HAp and brushite (DCPD), while tricalcium phosphate (TCP) is primarily synthesized using high-temperature methods [10]. An overview of the most important calcium phosphate phases can be found in [11–13]. It appears that brushite is a stable mineral during a large part of the reaction, but at the end of the reaction the pH reaches 7, thus above the stability window of brushite, which is between 2 and 6. The study of the ageing is thus important since brushite may transform into a more stable form.

3. Experimental procedure

3.1. Materials and Inorganic Phosphate Cement (IPC) synthesis

IPC is a two-component system, consisting of a calcium silicate powder and a phosphate acid-based solution of metal oxides [7]. As powder component, Wollastonite (CaSiO3) NYAD®200 of NYCO was used. The liquid mixture was a phosphoric acid solution, containing metal cations and a retarding agent following [14]. The weight ratio of powder to liquid used for all IPC mixtures in this research was 1/1.25, corresponding to a Ca/P ratio of 1.23. The two components of the IPC were mixed for five minutes at a speed of 1500 rpm with a blade mixer, in order to obtain a homogeneous mixture. The mixture was poured slowly, while being vibrated, into polycarbonate moulds. After the mould was filled, it was sealed by tape and left for 24 hours at ambient conditions, during which period the material sets. After that, the plates of IPC were removed from the mould, wrapped in a plastic foil and put in an oven at 60 °C for another 24 hours for further post curing. The last step was preparing the specimens for the mechanical tests by cutting them to the desired shape and dimensions. These new specimens were referred to as “reference specimens” in this research. This definition indicates that these specimens were not yet exposed to ageing, heating or any other treatment.

3.2. Heat exposure procedure (bulk specimens)

The effect of heating on the properties of IPC was determined after exposing bulk specimens to various temperatures. All subsequent tests were performed at room temperature. The following heat exposure procedure was used in this research:

1. The zero measurements (reference) were recorded immediately after curing at room temperature for 24 hours.
2. The test specimens were placed in the oven.
3. The oven was brought to the required temperature.
4. The required temperature was maintained during the specified period of time (usually 24 hours).
5. After the exposure period, the specimens were removed from the oven, weighed, and then brought back to ambient temperature before further testing.
6. The properties of interest were measured (e.g. weight, length, stiffness ….).
7. After placing the same specimens in the oven, the temperature was increased to the next required temperature and steps 4 to 7 were repeated with the same specimens until the highest required temperature (usually 300 °C or 1000 °C) was reached.

The test specimens (e.g. dimensions, shape …) were prepared according to the appropriate test method(s) for the evaluation of any exposure effects on the relevant product characteristics as specified. Moreover, to obtain more accurate values, at least three specimens were used for each test, with their average measurements used for analysis. The specimens were examined visually before and after each exposure step. Any visual exposure effects were recorded. Afterwards, the differences in appearance of the test specimens before and after exposure was observed, compared and recorded. Finally, the changes in the relevant characteristics were plotted or compared as a function of temperature.

3.3. Ageing

The reference specimens were aged for different periods at ambient conditions without any sealing.

3.4. Analytical techniques

3.4.1. Impulse Excitation Technique (IET)

The stiffness of the specimens was measured by using the Impulse Excitation Technique (IET). In this investigation, specimens with dimensions $15\times30\times320$ mm^3 were prepared to meet the requirements of this technique [15]. The specimens were supported at the first bending resonance mode and struck by a small metallic stick at their centre. The fundamental resonant frequency was measured via a piezoelectric transducer in contact with the specimen. Further details on the test methodology and calculations were given in references [16,17].

3.4.2. Optical microscope

In this research, we restricted our study to the cracking patterns on the surface of the specimens. To detect the cracking, an ink solution was used to colour the specimen surface. An optical microscope was then used to scan the specimens, while a digital camera fixed to this microscope captures the images.

3.4.3. Compressive and three-point bending strength

The specimens were tested in three-point bending and in compression. Testing was performed at room temperature with an Instron universal testing machine model 1195. The bending specimen's dimensions were: height = 15 mm, width = 30 mm and length 160 mm, the distance between the supports was 120 mm and the speed of the machine head during testing was 0.1 mm/minute. Compression tests were performed on the failed bending specimens, placed on their side with a loading area = 40×15 mm^2 and height = 30 mm. The speed of the machine head during testing was 2 mm/minute. Some of the specimens were tested in the condition they reached after ageing (denoted as ‘dry’), while others were immersed in water until saturated (denoted as ‘immersed’).

3.4.4. Thermogravimetric analysis, thermomechanical and dynamic mechanical analysis

A TGA7 from PerkinElmer was used, purged with Helium. Powdered samples (~40 mg) were tested. The heating rate was 5 °C/min. A DMA7 instrument from PerkinElmer was used purged with Helium, with a quartz parallel plate probe (diameter 1 mm). A cube of $5\times5\times5$ mm^3 was tested.

3.4.5. XRD

X-ray diffraction (XRD) was carried out on powdered and non-powdered samples using a Siemens D5000 diffractometer, generating a Cu Kθ radiation with an applied voltage of 40 kV and a current of 40 mA. XRD scans were measured from 15° to 70° 2-theta at a scan rate of 2°/min.

3.4.6. Helium pycnometry

The skeletal density of the IPC specimens was determined using the Helium pycnometer (Micrometrics AccuPyc 1330). Four specimens of IPC were prepared for this testing. The first specimen was used as reference IPC, while the other three specimens were heated at 105 °C, 150 °C and 200 °C using the heat exposure procedure [see Section 3.2]. These specimens were crushed into aggregates with a size of around 4 mm. The first specimen (reference IPC) was placed under vacuum for 24 hours to remove the moisture. The other three specimens were dried in a convection oven at 105 °C for 24 hours. A 10-cm3 sample chamber was filled by the dried IPC aggregates. Afterward, the sample chamber was filled with helium gas and pressure was measured. The helium then enters another empty chamber and the pressure in both chambers was measured. The sample volume was calculated based on these pressures and then with the known weight of the sample, the density was calculated. The helium was able to fill all spaces and all but the smallest micropores open to the atmosphere.

3.4.7. Mercury intrusion porosimetry

An AutoPore IV Serie 9500 from Micromeritics was used. The samples were placed in a closed cell called Penetrometer and evacuated. After a low vacuum level was reached (around 3 kPa), the cell was filled with mercury and pressure was increased continuously to 400 MPa. The maximum pore diameter was 300 μm, the surface tension 0.485 N/m and the contact angle: 130°.

4. Results and discussion

4.1. Phase constituents of reference IPC

Since the phosphoric acid solution used in this work differs from the one used in the previous work [9], it was checked if the same reaction products were obtained. The X-ray diffraction (XRD) patterns of the powdered reference IPC sample (see Fig. 1) show peaks corresponding to brushite and remaining wollastonite. No other crystalline products are obvious. Since the P/Ca ratio is below unity, remaining wollastonite is expected.

The X-ray diffraction pattern (Fig. 1) displays diffraction lines due to the crystalline phases, but also a prominent high background is observed between 15 and 40° 2θ. The hump in the diffractogram implies the presence of amorphous silica and eventually residual amorphous calcium phosphates [9,10]. It can thus be concluded that to a first approximation, the reaction products are comparable to the ones obtained with the model system of previous work [9].

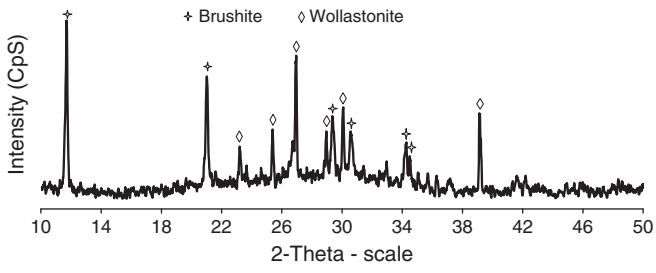

Fig. 1. Qualitative XRD patterns of reference IPC with crystalline peaks of brushite (B) and wollastonite (W).

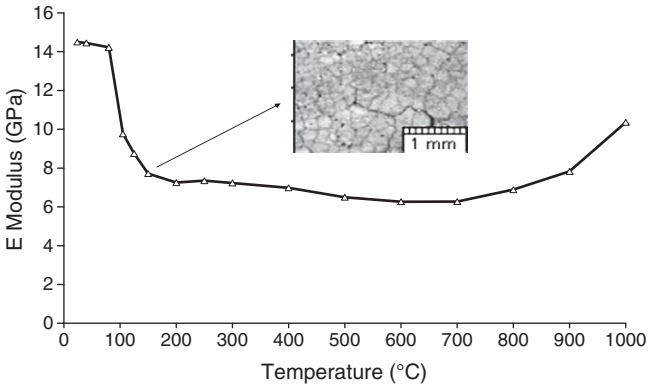

Fig. 2. Stiffness and cracking of IPC specimens as a function of temperature (IET and optical microscope).

4.2. Evaluation of mechanical properties and structural changes of IPC as a function of temperature

The variation of the stiffness with temperature, measured with the Impulse Excitation Technique, is plotted in Fig. 2. As the temperature increases from 80 °C to 200 °C, the specimens show a sharp drop in their stiffness: it is observed that the stiffness decreases by around 50%, from 14.2 GPa to 7.2 GPa, within the temperature range of 80 °C–200 °C. Images of the specimens' surface are taken with the optical microscope to detect the cracking in this temperature range. As a result of heating, map crack patterns are observed on the surface of the reference specimens at 105 °C, as shown in Fig. 2. Increasing the temperature further from 200 °C to 700 °C has only a limited effect on the stiffness of the IPC specimens. At temperatures between 700 °C and 800 °C, the stiffness starts to increase, as a result of reaching the glass transition temperature of some phases of the IPC, see Fig. 2.

Figs. 3 and 4 show the bending and the compressive strength of the IPC specimens after heating at various temperatures up to 1000 °C. Similar to the stiffness, the bending strength of dry specimens decreases sharply till around 105 °C and increases again at around 700 °C–800 °C. This indicates that cracking up to 105 °C and the effect of the glass transition temperature at about 800 °C are the major contributions to these variations. The bending strength of immersed specimens is almost the same as the bending strength of dry specimens at room temperature, but after heating at a temperature of 105 °C and higher, the wet strength is about twice as low as the dry one. The bending strength of the immersed specimens shows the same trend as the dry specimens as a function of temperature, Fig. 3. On the other hand, the observed microcracking has only a limited influence on the compressive strength, see Fig. 4: the increase in defect size has a more pronounced effect on a

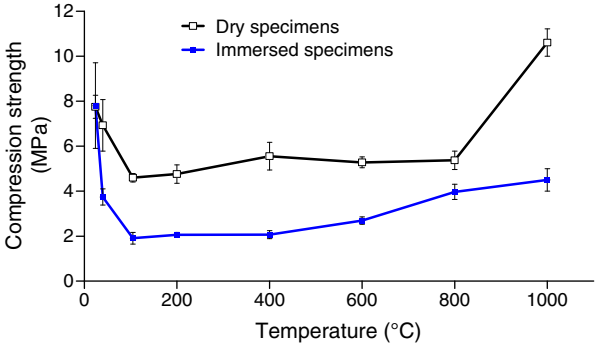

Fig. 3. Bending strength of IPC at room temperature after heating the specimens at different temperatures.

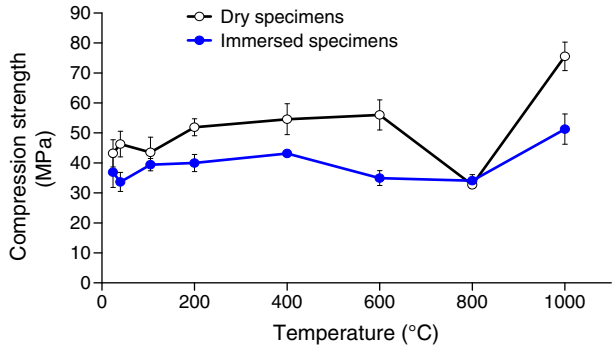

Fig. 4. Compressive strength of IPC at room temperature after heating the specimens at different temperatures.

Griffith type of failure. Compressive strength does not change notably by heating up to 600 °C. Exposure above 800 °C causes an increase in the specimen's compressive strength.

Based on the above results, we can conclude that the network of microcracks plays a major role in the reduction of IPC's mechanical performance after exposure to temperatures above 100 °C.

4.3. Evaluation of mass loss, shrinkage and phase changes of IPC as a function of temperature

To understand the behavior of the IPC at elevated temperature, a more fundamental study is carried out.

4.3.1. TGA and TMA (small samples, ~40 mg)

IPC might be used as a construction material in situations where elevated temperatures may occur. Its thermomechanical behavior is shown in Fig. 5. Some distinct shrinkage is observed in the first heating curve up to 850 °C. During a second heating none of these steps is reproduced and a normal expansion is seen. To understand the changes going on during the first heating, the weight loss is also measured over the same temperature interval. The derivatives of mass and length variations, obtained by TGA and TMA are also plotted in Fig. 5 to better visualize small steps. One can distinguish four steps in mass loss: the first one occurring from the beginning of the experiment (due to the evaporation of free water present in the material), the second one around 130 °C, the third one around 205 °C and the fourth one around 440 °C. Furthermore there are two steps of shrinkage observed above 515 °C without a corresponding loss of mass.

Next to amorphous silica, brushite is one of the main components of IPC. The dehydration of brushite is known to occur in several steps [18]. The crystal structure of brushite contains compact sheets, consisting of parallel chains, in which calcium ions are coordinated by six phosphate oxygen and two oxygen atoms belonging to the water molecules. Besides the adsorbed water molecules on its surface, two kinds of water molecules exist in brushite differing in the strength of the hydrogen bonding [19]: one (W1) is linked to the phosphate oxygen by strong hydrogen bonds, whereas the other one (W2) presents longer and weaker hydrogen bonds.

The dehydration of the reference IPC was also studied by XRD, showing the appearance of monetite after heating to 150 °C for 1 day. We can summarize the transformation of brushite to monetite (Eq. 2) in the following two statements: 1) The removal of W1 between 105 °C and 150 °C transforms brushite into an intermediate phase 2) Heating to temperatures above 220 °C causes the complete dehydration of the intermediate phase, into monetite. Also for amorphous calcium phosphates (ACP), it is reported that there are different types of water: 1) adsorbed water which evaporates under 105 °C and 2) hydrate water [18]. The free and adsorbed water is released continuously, Fig. 6.

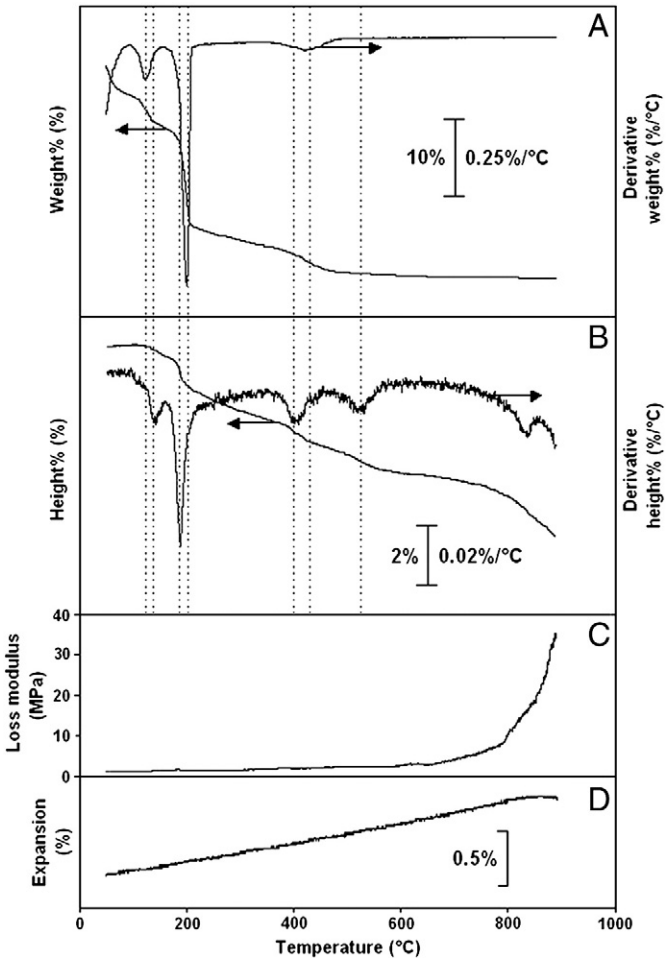

Fig. 5. Thermograms of TGA and DMA of reference IPC: A) weight loss and the derivative of the weight loss, B) shrinkage and the derivative of the shrinkage, C) loss modulus obtained by DMA analysis, and D) expansion of the material during a second scan in the DMA analysis. The vertical dotted lines indicate the temperatures where the mass losses or the height changes are observed.

ACP as an amorphous phase loses its bound hydrate water in a broad temperature range [18]. The loss of mass resulting from the dehydration of ACP's free, adsorbed and hydrate water can probably also be observed in Fig. 6 as part of the continuous weight loss below 200 °C.

$$CaHPO_4.2H_2O \rightarrow CaHPO_4 + 2H_2O \quad (2)$$

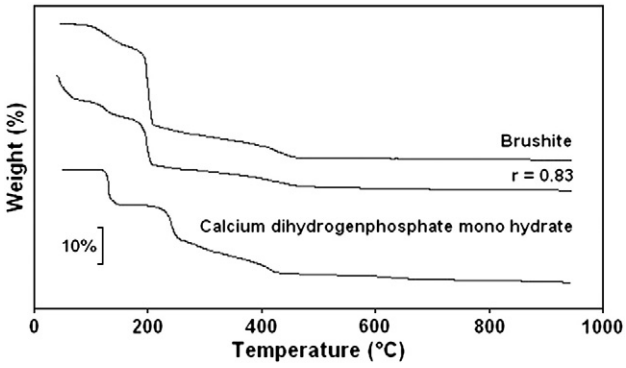

Fig. 6. TGA thermograms of reference IPC (r = 0.83), pure brushite and pure calcium dihydrogenphosphate mono hydrate. The mass at a temperature of 550 °C is used as a reference mass (= 100%). The curves are shifted for clarity.

$$2\,CaHPO_4 \rightarrow Ca_2P_2O_7 + H_2O \quad (3)$$

The next distinct mass loss was observed between 390 °C and 515 °C, see Fig. 5. This can be ascribed to the decomposition of monetite into calcium pyrophosphate ($Ca_2P_2O_7$) and H_2O (see Eq. 3) around 440 °C according to TGA [20]. The same evolutions are observed by means of XRD at more or less the same temperatures.

The dehydration of brushite ($CaHPO_4.2H_2O$) in the temperature range 80 °C–450 °C is reflected in the shrinkage pattern as seen in Fig. 5. At about 500 °C, just after the last weight loss, a next shrinkage step is observed. Starting from 700 °C, the material seems to shrink again. The loss modulus measured with DMA, starts to increase in this temperature interval, pointing to the softening of the material. The last 'shrinkage' observed is thus rather due to viscous flow than 3-dimensional shrinkage. At this moment it is not clear yet whether this transition is due to the silica phase or to one of the calcium phosphate phases.

XRD helps to further elucidate the structural changes (Fig. 7). The intensity of the signals at the typical diffraction angles of monetite diminish and disappear at 470 °C. Starting from 470 °C a new crystalline component is formed. From 650 °C on the presence of calcium pyrophosphate is very clear. The structural rearrangements, and especially the crystallization, probably cause the shrinkage at 500 °C. In addition to calcium pyrophosphate ($Ca_2P_2O_7$), some other XRD peaks corresponding to new crystalline CaP phases, possibly $Ca_4P_6O_{19}$ and CaP_4O_{11}, at this temperature can be observed, Fig. 8. No information about a possible transition in the amorphous silica could be obtained. Nevertheless, such a transition may possibly happen because the glass transition temperature of amorphous silica may be exceeded. Pure amorphous silica has a glass transition temperature of about 1200 °C [21–23]. When hydrogen or metal ions are present in the amorphous phase, its glass transition temperature decreases. In the formed materials, hydrogen and calcium atoms (remaining in the amorphous structure that was originally wollastonite) can cause a drop in the glass transition of the silica phase, possibly below 1000 °C. If the temperature rises above the glass transition, structural changes are possible.

4.3.2. Porosity and pore structure

Fig. 9 presents a typical mercury intrusion porosimetry (MIP) result on reference IPC. Two measurements on different reference samples are plotted to show the reproducibility. The incremental volume versus pore diameter shows only one peak, centered at 20 nm, indicating the presence of mesopores in the sample. Such results certainly indicate a very limited amount of macropores (greater than 0.1 μm), ~1% of the total volume, in the reference specimens. Remark however that large cracks and voids cannot be measured with this technique. According to mercury intrusion porosimetry the total porosity of IPC is around 30%.

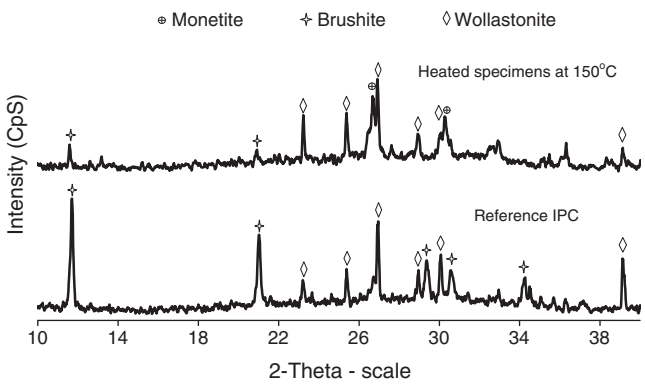

Fig. 7. Qualitative XRD patterns of reference IPC and after heating at 150 °C for 24 hours (powder specimens).

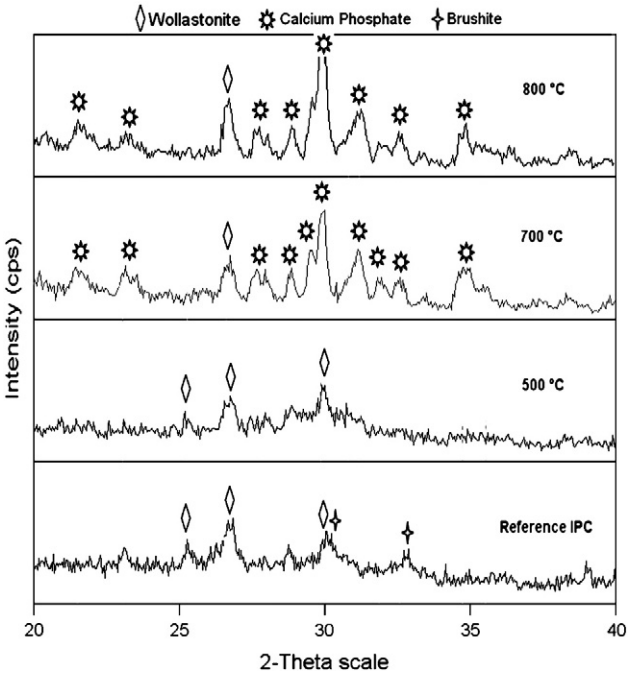

Fig. 8. XRD spectra of IPC heated up to the temperature mentioned.

Fig. 10 A illustrates the cumulative distribution of the pores and the total pore volume in the reference IPC in these scenarios: at room temperature, after heating it at 110 °C and after heating it at 150 °C. The regions of the mesopores and the macropores are separated by a dotted line. The derivatives of pore distributions of these specimens are shown in Fig. 10B. These results show that the relative amount of macropores increases from 1% to 16% when heated from room temperature to 150 °C.

4.3.3. Mechanism of the thermal IPC shrinkage resulting from phase transformations

IPC shrinkage is of increasing concern when focusing on maintaining durable structures with composite materials at elevated temperatures. Although chemical transformations take place at certain temperature ranges, they depend also on ageing and pore moisture. At temperatures even below 105 °C the shrinkage induces cracking which can severely decrease IPC life expectancy. These dimensional changes are mainly attributed to evaporation of water without phase transformation.

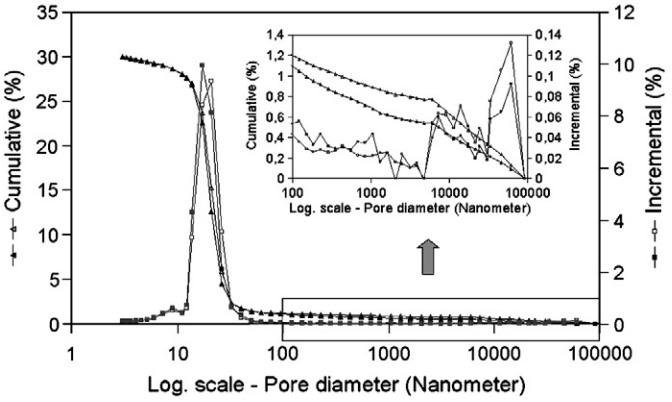

Fig. 9. Pore size distributions of two reference IPC specimens obtained by using MIP technique (percentage of the total specimen's volume).

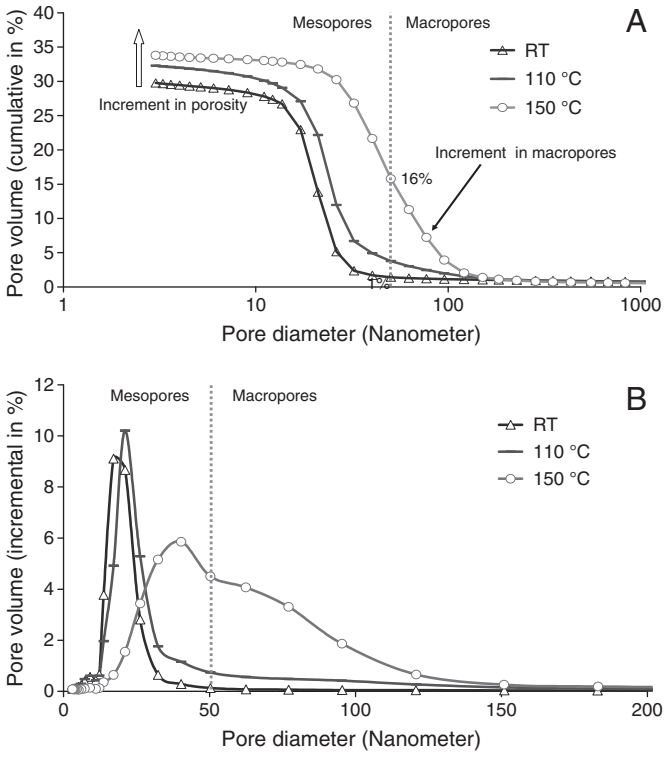

Fig. 10. Distribution of pore sizes of IPC as a result of heat treatment (MIP), A. Cumulative in %, B. Incremental in %.

Subsequently high bulk shrinkage occurs simultaneously with little changes in skeletal density measured via helium pycnometry as shown in Fig. 11. The chemical transformations of the calcium phosphates above 105 °C cause compaction in the structure of the phases (local shrinkage) as well as the bulk structure of the IPC (bulk shrinkage), Fig. 12. The transformation of brushite (with skeletal density 2.32 g/cm^3) to monetite (with skeletal density 2.89 g/cm^3) is the main factor behind the shrinkage in IPC in the temperature range of 105 °C to 220 °C. Local shrinkage occurs only in the shrinking phases of the solid skeleton, in the first place brushite and ACP and possibly also amorphous silica. The non-shrinking phase, residual wollastonite, also influences the development of internal stresses because of the differential shrinkage between the non-shrinking and shrinking phases. Therefore, the prediction of bulk shrinkage depends on the shrinking phases, the non-shrinking phase and the pore phase. The bulk structure of IPC is composed out of a solid skeleton,

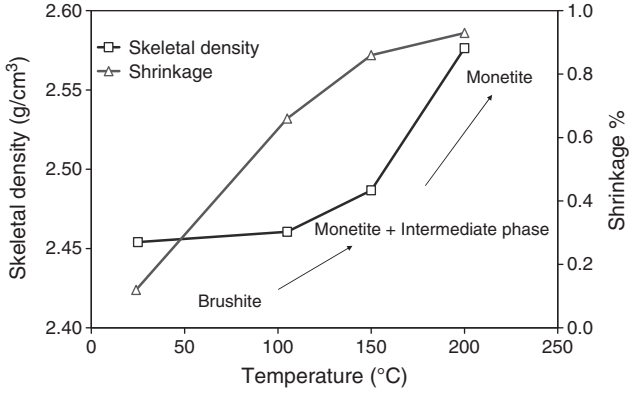

Fig. 11. Shrinkage and corresponding skeletal density of IPC as function of temperature (Helium pycnometer).

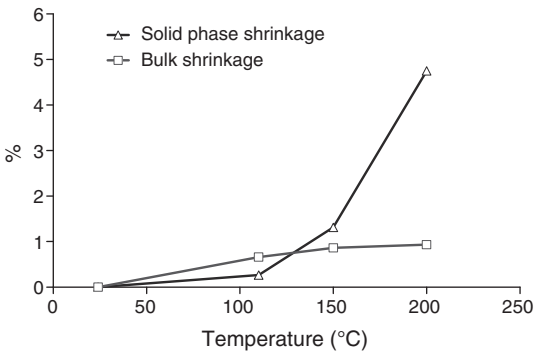

Fig. 12. Shrinkage of solid phase and bulk structure of IPC with heating up to 200 °C.

water phases and a pore system. The variations of this structure as a function of temperature are rather complex. Fig. 10 shows that pore size distribution of IPC is a function of temperature. Accordingly, a case study of the bulk structure of IPC is discussed as a function of temperature up to 200 °C.

Fig. 12 illustrates the shrinkage of the solid skeleton and the shrinkage of the IPC (bulk shrinkage). Pore size distributions of the first three specimens (room temperature, 110 °C, and 150 °C) are presented already in Fig. 10. Limited changes take place in skeletal density and pore system in the temperature range RT — 110 °C. Accordingly, we will focus on the changes that take place in the temperature range of transformation of brushite to monetite: 110 °C to 200 °C. Significant shrinkage occurs in the solid phase when brushite transforms into monetite and into an intermediate phase at a temperature range of 110 °C to 150 °C. In this temperature range, bulk shrinkage continues, but at a lower rate than observed at the room temperature to 110 °C range. Increasing the temperature up to 200 °C further dehydrates the IPC and transforms most of the brushite to monetite. A strong discrepancy is observed between the skeletal density increasing much faster than the corresponding bulk shrinkage which hardly changes. Since the strong compaction of the solid phase (skeletal density) is not observed on the external dimensions this implies that the porosity still increases.

4.4. Ageing effects on the mechanical properties of IPC

Three groups of IPC specimens are prepared, and the effects of ageing at ambient conditions on their strength are evaluated. The first group is subjected to three point bending and compression tests seven days after post curing; the second group is aged at ambient conditions for 12 months before the same tests are conducted; and the last group is aged for 20 months before undergoing the tests. Fig. 13 illustrates

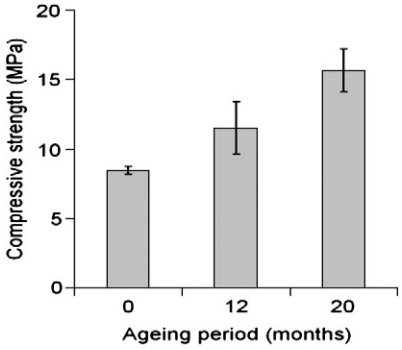

Fig. 13. Increment in bending strength of IPC after ageing at ambient conditions for 12 and 20 months.

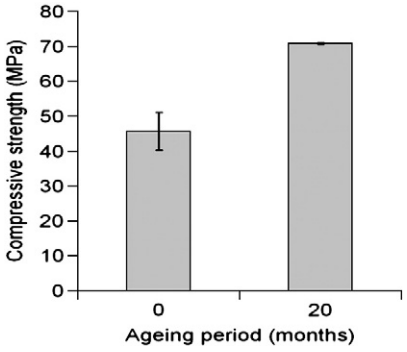

Fig. 14. Increment in compression strength of IPC after ageing at ambient conditions.

the bending strength of non-aged and aged specimens. It is observed that the average bending strength of the IPC increases 1.4 times by ageing at ambient conditions for 12 months and nearly doubles when the ageing period is increased to 20 months. The compressive strength of such a specimen also increases 1.5 times as shown in Fig. 14. These changes in the mechanical properties of IPC over time are probably related to the changes observed after the transformation of brushite, as shown in Fig. 7.

4.5. Evaluation of ageing effects on the mass loss, shrinkage and phase changes of IPC

4.5.1. TGA and TMA (small samples, ~40 mg)

Fig. 15 illustrates the redistribution of the IPC's bound water, with ageing time. Specimens that are not subjected to post curing, Fig. 15B, show the highest release of bound water and physico-chemically bound water between 80 °C and 130 °C, while aged specimens exhibit the lowest degree of dehydration and evaporation. A shift in the relative amount of W2 to W1 is observed by post curing and ageing. This increment in W1 is an indication of increment in brushite phase over time, which might be a result of continuation of the chemical reactions, especially the transformation of wollastonite to brushite and/or crystallization of ACP to form brushite. The shrinkage shows a comparable evolution, with a shift to higher temperatures and an increasing shrinkage at 215 °C (W1). The formation of more calcium phosphates (e.g. brushite and ACP) contributes to the ongoing reactions, and they play a major role in the recovery of the mechanical properties of the IPC after ageing. This was clearly shown in Section 4.4.

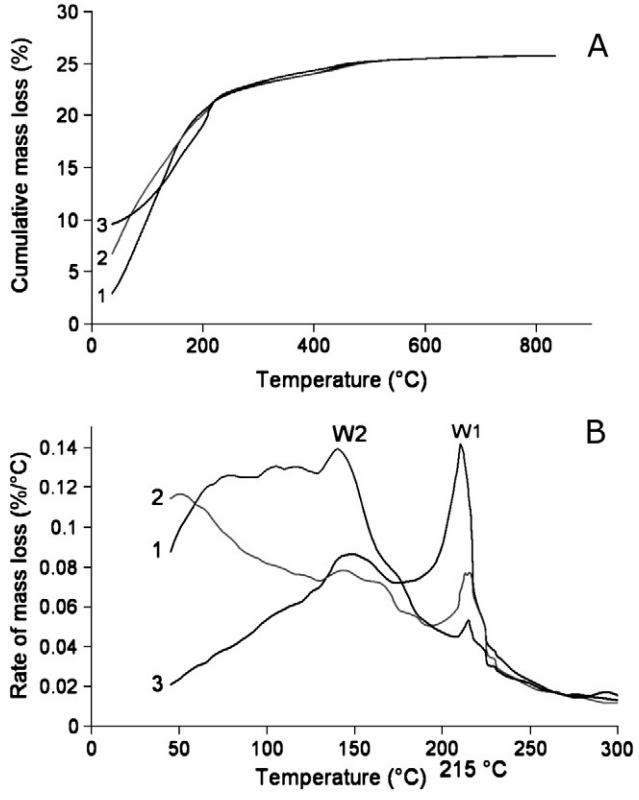

Fig. 15. Redistribution of IPC bound water by post curing and ageing for 20 months (TGA) A. Heating to 900 °C; B. derivative of weight loss curves up to 300 °C; (1) specimens without post curing; (2) Reference specimens; (3) Aged specimens for 20 months.

4.5.2. Crystalline phases

To detect the formation of new chemical phases as a result of transformations over time XRD patterns are obtained on specimens aged for different periods up to 20 months at ambient conditions (Fig. 16). In general, the XRD patterns in Fig. 16 do not indicate that the IPC exhibit new crystalline phases or phase transformations after 20 months of ageing at ambient conditions. From these diffractograms it is also not clear if the relative amount of wollastonite, brushite and monetite changes. Further studies on the behavior of bound water in IPC need to be conducted to allow for a more thorough understanding of structural changes and shrinkage under the effects of ageing.

5. Conclusion

The Inorganic Phosphate Cement studied is composed of brushite, some amorphous Ca-phosphate, amorphous silica and remaining wollastonite. During heating of the Inorganic Phosphate Cement, different transitions are observed:

- The dehydration from brushite to monetite (till 220 °C)

$$CaHPO_4.2H_2O \rightarrow CaHPO_4 + 2H_2O$$

- The dehydration from monetite to calcium pyrophosphate (till 415 °C)

$$2CaHPO_4 \rightarrow Ca_2P_2O_7 + H_2O$$

- Possible (re)crystallization (above 500 °C) glass transition of one of the phases of the material (at about 800 °C)

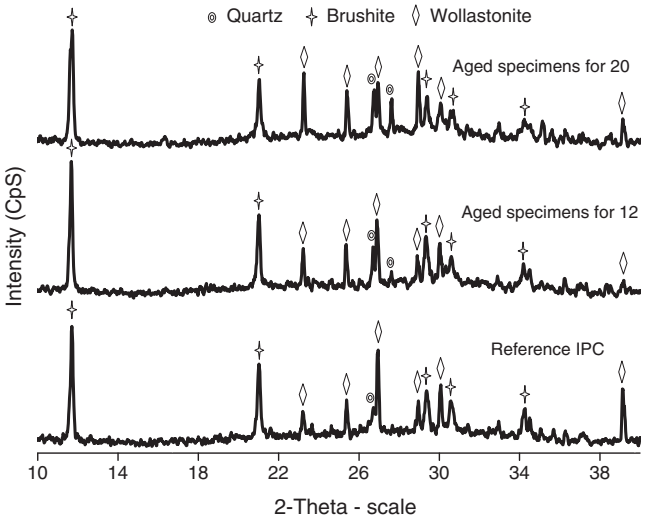

Fig. 16. XRD pattern of specimens after ageing for 20 months (powdered samples).

The dehydration of brushite and the crystallization cause shrinkage of the material. Since not all of the phases shrink, this introduces stress and cracks. The skeleton density even increases more than the bulk density, resulting in an increased porosity. The initial pore size distribution is narrow and centered at about 20 nm. The pore size distribution of the heat treated IPC (150 °C) is however much broader and shifted to larger values.

The cracking explains the decreased bending strength of heat treated IPC up to 700 °C, which is only about half of the strength of the reference specimens. The compression strength is not influenced by this effect. At higher temperatures the strength increases again due to the healing effect of the glass transition.

As a result of ageing of IPC at ambient conditions the meta-stable calcium phosphate phases, brushite and amorphous calcium phosphate, dehydrate partially. Also the chemical reactions continue even after the substance has set. These ongoing chemical transformations and reactions over time contribute significantly to the enhancement of the material's mechanical properties. It has been established that ageing the IPC for 20 months at ambient conditions doubles its bending strength and increases its compressive strength by 50%. An attempt was done to study the molecular changes at the base of the ageing effects observed in mechanical strength. However, XRD did not reveal any more pronounced crystallization or the formation of a new crystalline component.

This article shows that several challenges arise when using IPC for construction and other industrial applications, in particular for high temperature applications. These challenges include shrinkage, early cracking and ageing effects. In another article we will present a post curing technique to overcome these shortcomings and to obtain an end product with an improved dimensional and thermal stability.

References

[1] A. Tofighi, K. Schaffer, R. Palazzolo, Calcium phosphate cement (CPC): a critical development path, Key Engineering Materials Vols. 361–363 (2008) 303–306.
[2] L. Sun, H.H.K. Xu, S. Takagi, C. Chow, Fast setting calcium phosphate cement-chitosan composite: mechanical properties and dissolution rates, Journal of Biomaterials Applications Vol. 21 (3) (2007) 299–315.
[3] S.C. Liou, S.Y. Chen, H.Y. Lee, J.Sh. Bow, Structural characterization of nano-sized calcium deficient apatite powders, Biomaterials Volume 25 (Issue 2) (January 2004) 189–196.
[4] W.E. Brown, L.C. Chow, A new calcium phosphate setting cement, Journal of Dental Research 62 (1983) 672.
[5] W.D. Kingery, Cold setting properties, Journal of the American Ceramic Society 33 (8) (1950) 242–247.
[6] B. F.Lautre, M. D.Escamps, C. DElecourt, M.C. BLary, P. HArdouim, Journal of Materials Science: Materials in Medicine 12 (2001) 679.
[7] H. Cuypers, J. Wastiels, Thin and strong concrete composites with glass textile reinforcement: modeling the tensile response, American Concrete Institute Special Publication SP-250, 2008, pp. 131–148.
[8] H. Cuypers, "Analysis and design of sandwich panels with brittle matrix composite faces for building applications", PhD thesis, Vrije Universiteit Brussel (VUB), Belgium 2002.
[9] G. Mosselmans, M. Biesemans, R. Willem, J. Wastiels, M. Leermakers, H. Rahier, S. Brughmans, B. Van Mele, Thermal hardening and structure of a phosphorus containing cementitious model material phosphoric acid–wollastonite, Journal of Thermal Analysis and Calorimetry Vol. 88 (3) (2007) 723–729.
[10] A.L. Oliveira, R.L. Reis, Pre-mineralisation of starch/polycrapolactone bone tissue engineering scaffolds by calcium-silicate-based process, Journal of Material Science: Materials in Medicine 15 (2004) 533–540.
[11] P. Kumta, C. Sfeir, D. Lee, D. Olton, D. Choi, Nanostructured calcium phosphates for biomedical applications: novel synthesis and characterization, Acta Biomaterialia 1 (2005) 65–83.
[12] E. van der Wal, "Bioactivity and surface reactivity of RF-sputtered calcium phosphate thin films", PhD thesis, Universiteit Utrecht, Katholieke Universiteit Nijmegen, Holland, 2003.
[13] S.V. Dorozhkin, M.E. Epple, Biological and medical significance of calcium phosphates, Angewandte Chemie International Edition 41 (2002) 3130–3146.
[14] EP 0 861 216, "Inorganic Resin Compositions, their Preparation and Use thereof".
[15] T. Lauwagie, H. Sol, G. Roebben, W. Heylen, Y. Shi, Validation of the resonalyser method: an inverse method for material identification, Publications at ISMA (International Conference on Noise and Vibration Engineering), September 2002, pp. 687–694.
[16] G. Pickett, Equations for computing elastic constants from flexural and tensional resonant frequencies of vibration of prisms and cylinders, ASTM Proceedings 45 (1945) 846–865.
[17] A. Wolfenden, et al., Dynamic Young's modulus measurements in metallic materials: results of an interlaboratory testing program, Journal of Testing and Evaluation (Jan 1989) 2–13.
[18] M. Sedlak, A. Beebe, Temperature programmed dehydration of amorphous calcium phosphate, Journal of Colloid and Interface Science volume 47 (Issue 2) (May 1974) 483–489.
[19] L. Tortet, J.R. Gavarri, G. Nihoul, Study of protonic mobility in CaHPO4·2H2O (brushite) and CaHPO4 (monetite) by infrared spectroscopy and neutron scattering, Journal of Solid State Chemistry 132 (1997) 6–16 article no. SC977383.
[20] S. Brughmans, Physical-chemical characterization of a model system for inorganic phosphate cement, department of chemical Engineering, Vrije Universiteit Brussel, 2003.
[21] S.K., A.J. Ikushima, Applied Physics Letters 70 (3504) (1997).
[22] W.K., K. Mukai, ISIJ International 43 (606) (2003).
[23] R. Brüning, Journal of Non-Crystalline Solids 330 (2003) 13.